

# Coupled quadrupole-phonon excitations in CeAuAl<sub>3</sub> and spin wave excitations in MnWO<sub>4</sub>

B.-Q. Liu<sup>1,2</sup>, P. Čermák<sup>2</sup>, A. Schneidewind<sup>2</sup>, and Sohyun Park<sup>3</sup>

<sup>1</sup>Key Laboratory of Neutron Physics, Institute of Nuclear Physics and Chemistry, CAEP, Mianyang, PR China

<sup>2</sup>Jülich Centre for Neutron Science (JCNS) at MLZ, Forschungszentrum Jülich GmbH, Garching, Germany

<sup>3</sup>Section Crystallography, Department for Earth and Environmental Sciences, Ludwig-Maximilians-Universität München, Theresienstrasse 41, 80333 Munich, Germany

## Structural properties and lattice dynamics of CeAuAl<sub>3</sub>

### Introduction and Motivation:

✓ Ce-based heavy fermion intermetallic compounds CeTX<sub>3</sub> (*T*: transition metal, X= Si, Ge, or Al)

✓ Weak magnetoelastic interaction can lead to the anticrossing phenomenon in inelastic neutron scattering experiments.

✓ Strong magnetoelastic interaction can lead to the formation of a bound state between phonons and crystal field (CEF) excitation, which can not be explained by a pure CEF model.

**Computational method:** DFT calculations have been carried out with the PAW method, GGA descriptions for the exchange-correlation functional. The cutoff energy is set as 500 eV in plane-wave basis expansion. The *k*-point meshes are sampled by 14 × 14 × 7 according to the Monkhorst-Pack scheme.

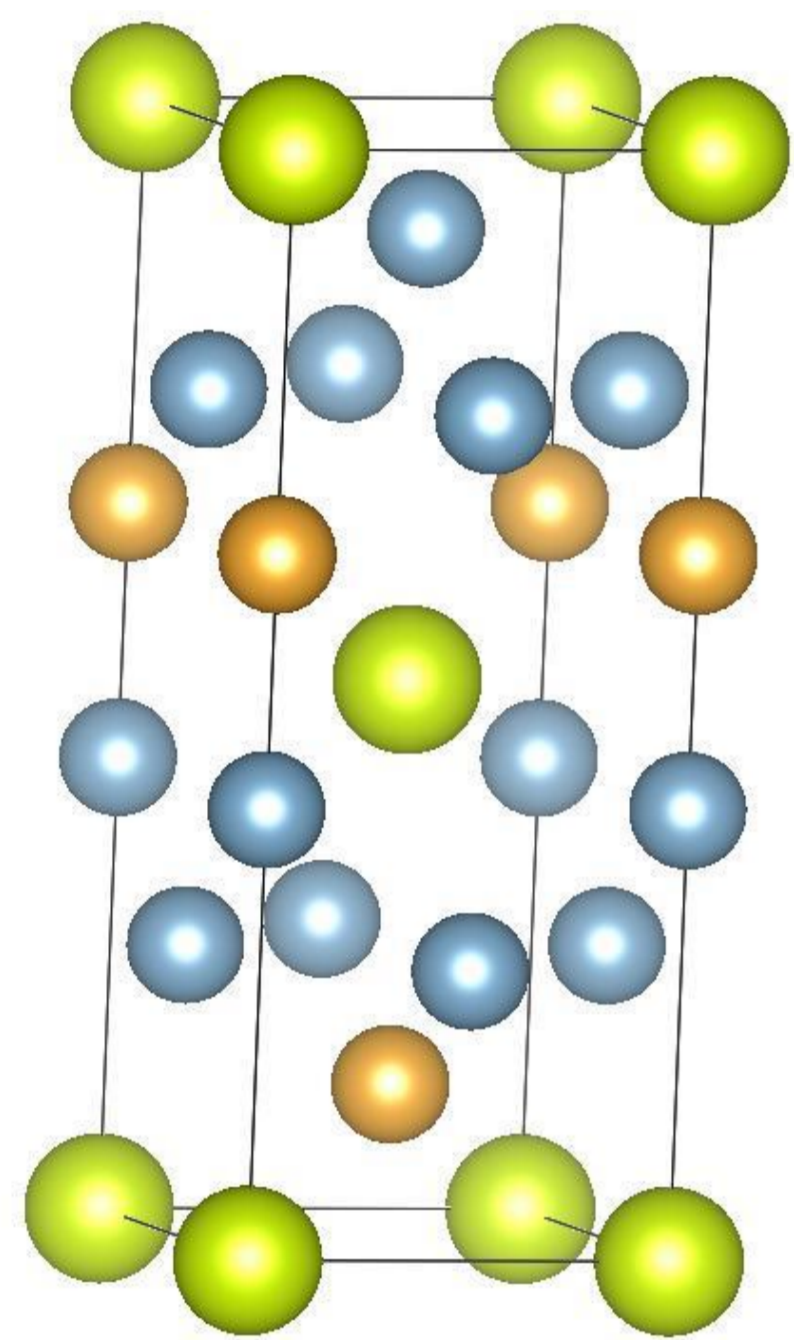


FIG. 1 Crystal structure of CeAuAl<sub>3</sub>, with Ce in yellow, Au in orange, Al in blue.

The phonon calculations are performed with the finite difference method. A 2 × 2 × 2 supercell was constructed and Phonopy was used. Phonon dispersion along  $\Gamma$ -Z- $\Sigma$ - $\Gamma$  is shown in FIG. 2. The irreducible representations for the high symmetry points are:  $\Gamma=4r_1+r_3+5r_5$ ,  $Z=4r_1+r_3+5r_5$ , and  $\Sigma=9A'+6A''$ , respectively.

Table 1. Structural parameters for CeAuAl<sub>3</sub>.

	<i>a</i> (Å)	<i>c</i> (Å)	<i>c/a</i>	<i>V</i> <sub>0</sub> (Å <sup>3</sup> )
Expt. at 300 mK <sup>[1]</sup>	4.3105	10.7965	2.5047	200.60
Expt. at 9 K <sup>[1]</sup>	4.3172	10.8090	2.5037	201.46
Expt. [2]	4.3364	10.85	2.5021	204.03
Our DFT study	4.3354	10.8436	2.5012	203.81

**Summary:** The magnetoelastic interaction which is not strong will lead to mixed-mode excitations of phonons and quadrupole excitations in CeAuAl<sub>3</sub>.

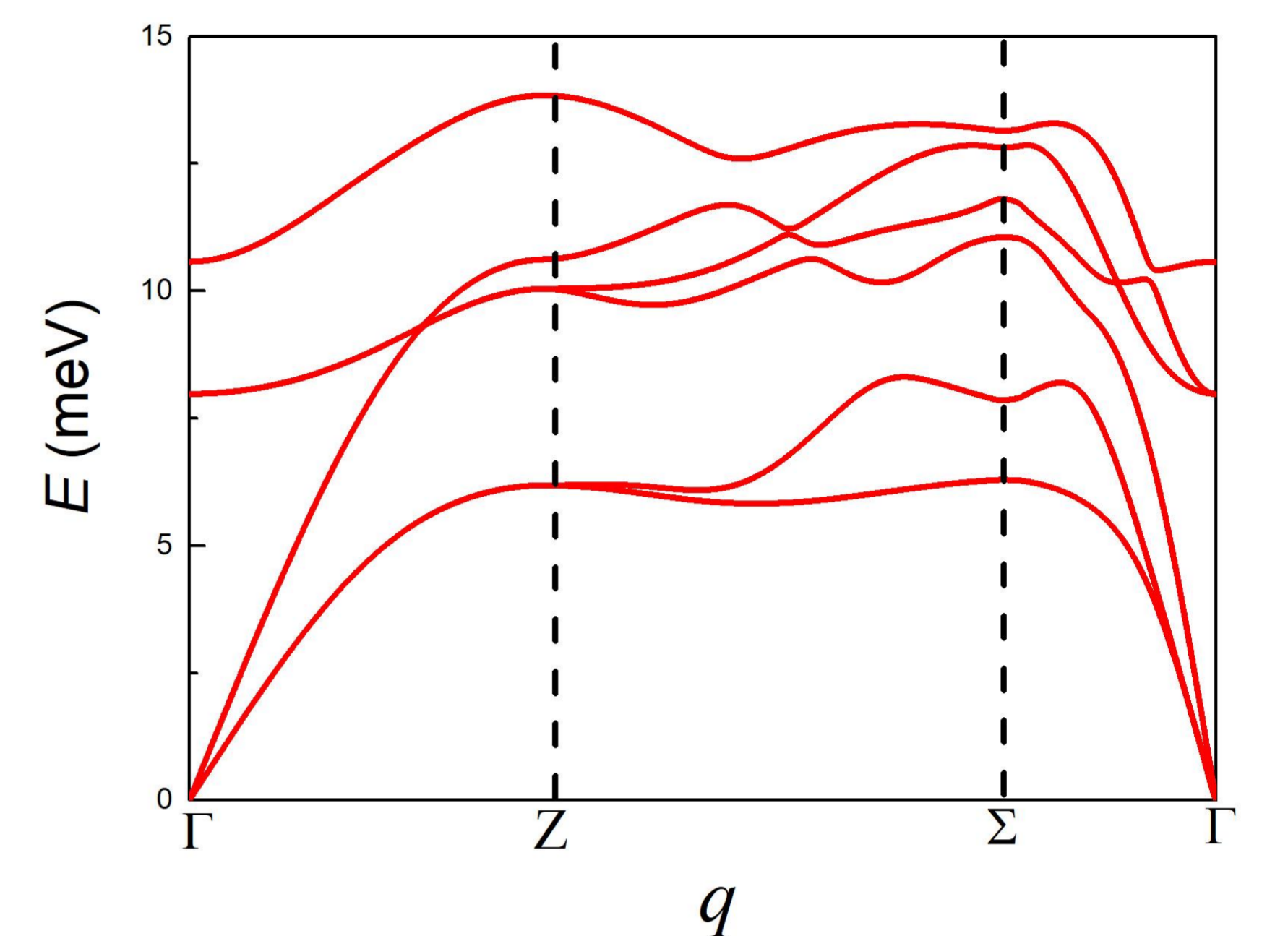


FIG. 2 Phonon dispersion for CeAuAl<sub>3</sub> along high symmetry lines  $\Gamma$ -Z- $\Sigma$ - $\Gamma$ .

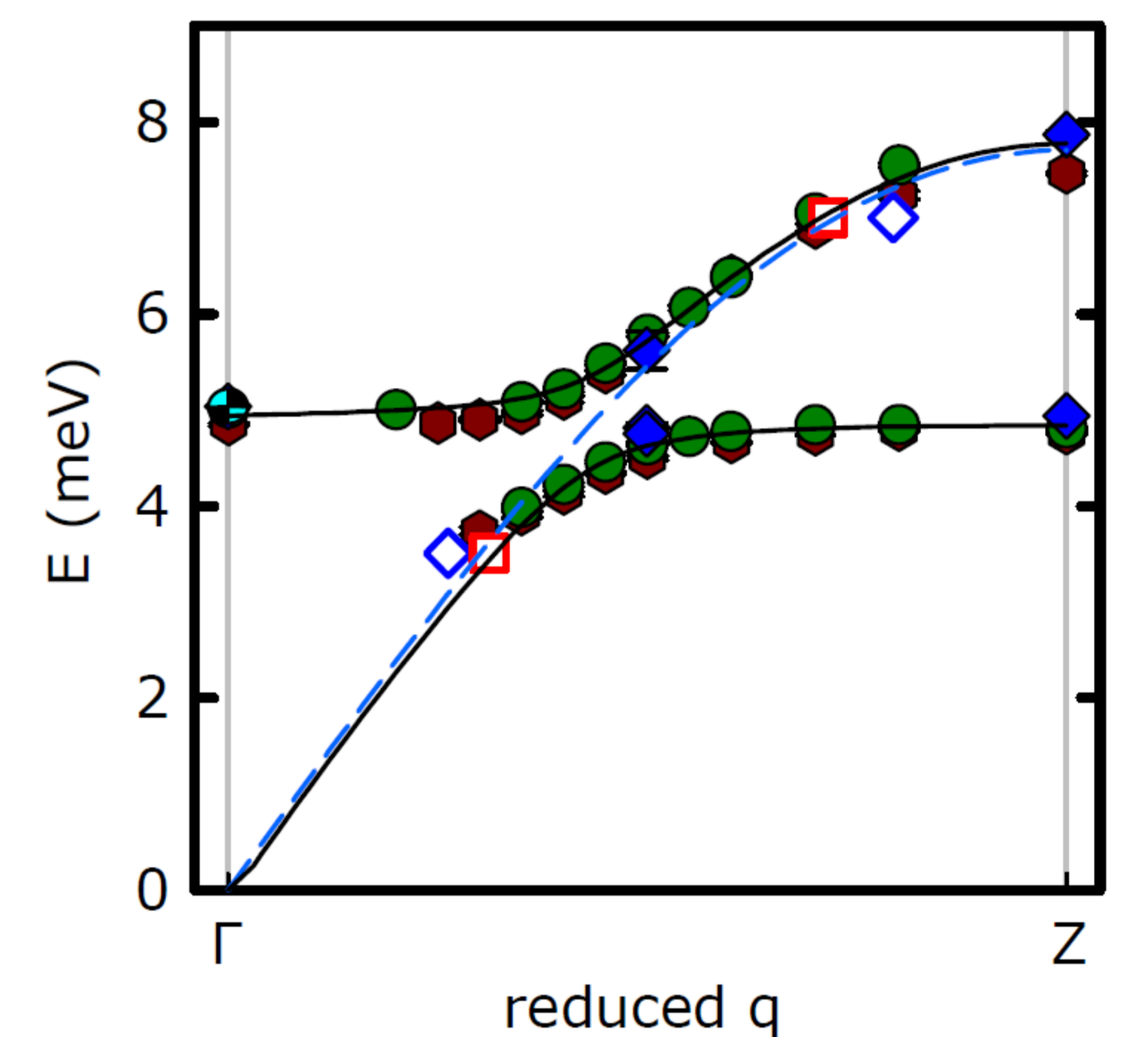


FIG. 3 Dispersion curves of the coupled excitations in CeAuAl<sub>3</sub> [3].

## Two spin-canting textures in the AF1 phase of multiferroic MnWO<sub>4</sub>

### Introduction and Motivation:

✓ an exemplary prototype of magnetoelectric control, possible applications like data storage, magnetoelectric sensors

✓ a promising system for the study of magnetic phase transitions and related critical phenomena

✓ rich magnetic phase diagram by chemical substitutions and applying magnetic fields

✓ competing long-range exchange coupling

**Computational method:** Total energies of both collinear (Fig. 4a) and non-collinear (Fig. 4b) AF1 models have been calculated within the PAW method, GGA descriptions for the exchange-correlation functional. The cutoff energy is 500eV in plane-wave basis expansion. A supercell with 216 atoms has been constructed, using only the  $\Gamma$ -point for *k*-point integrations.

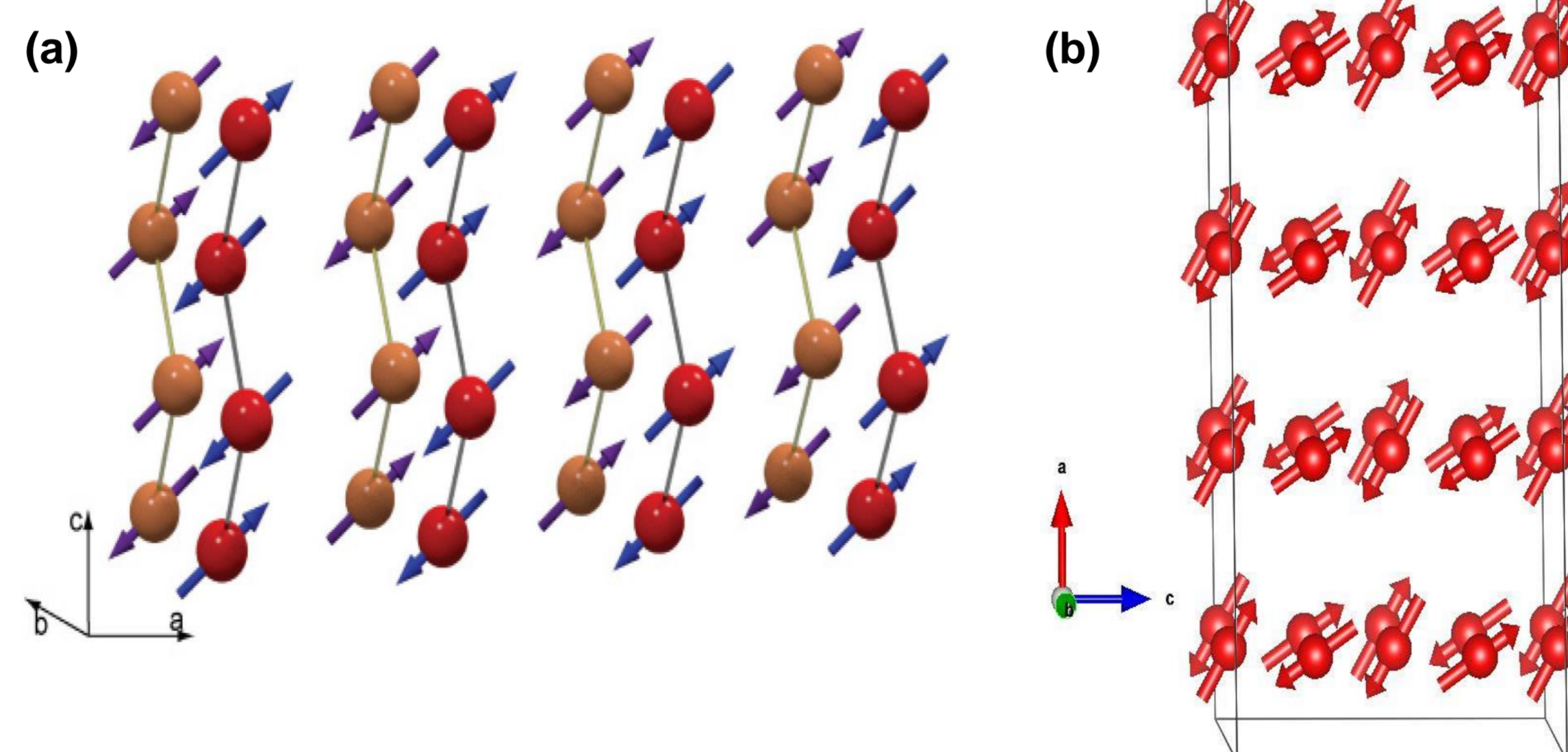


FIG. 4 The magnetic model of the AF1 phase of MnWO<sub>4</sub>, (a) collinear, taken from Ref.[4], (b) non-collinear, displaying only the magnetic Mn<sup>2+</sup> ions.

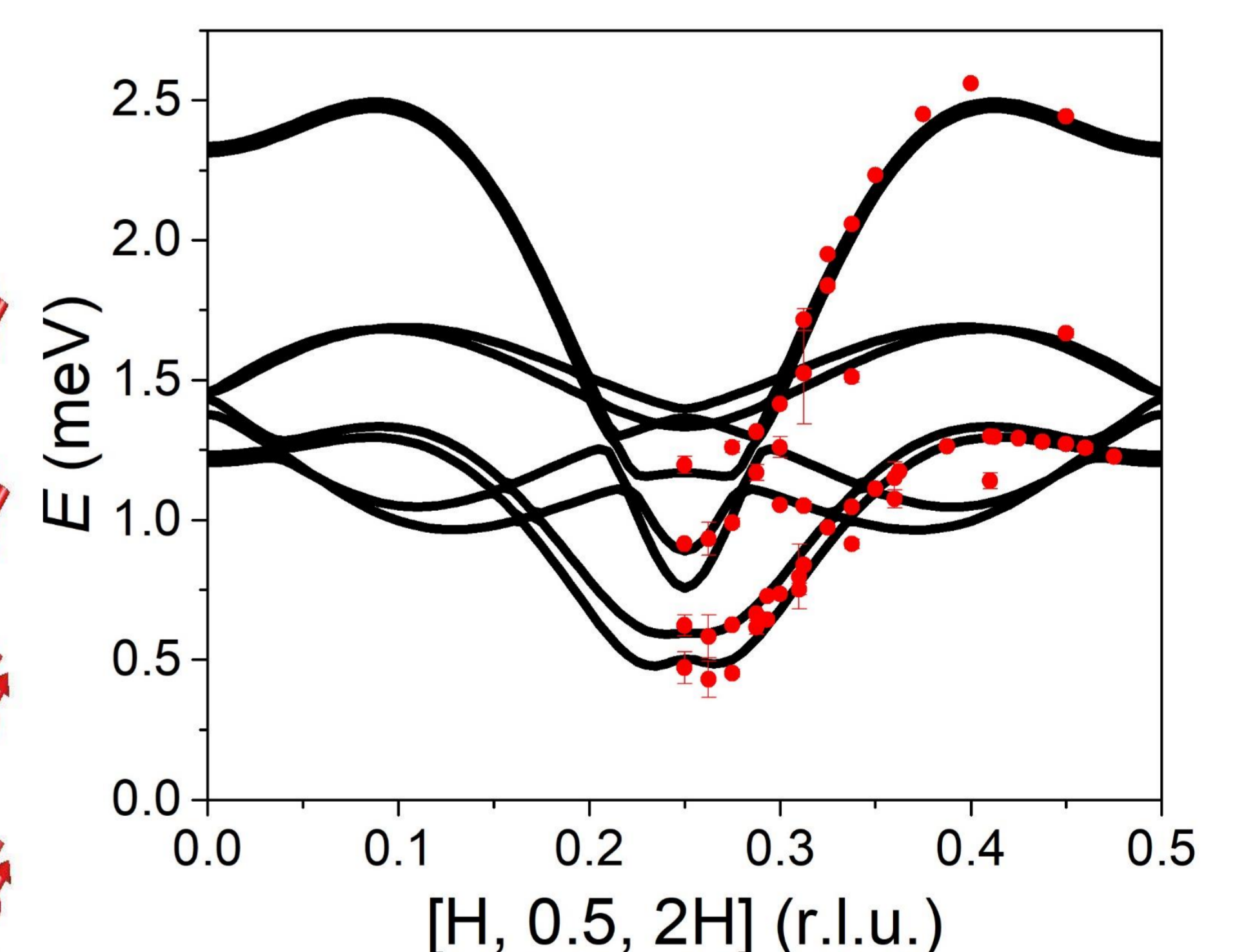


FIG. 5 The spin wave dispersion of the AF1 phase of MnWO<sub>4</sub>, the red circles are experimental data taken from Ref.[5], fitted by the non-collinear model.

**Summary:** The energy of the two spin-canting structure is lower than that of the collinear model, i.e., the ground state of MnWO<sub>4</sub> prefers two spin-canting textures. Besides, the lowest spin wave branch can be properly described by the spin-canting model while the collinear model with one single-ion anisotropy parameter failed.

[1] D. T. Adroja, C. de la Fuente, A. Fraile, *et al.*, PRB **91**, 134425 (2015).

[2] C. Franz, A. Senyshyn, A. Regnat, *et al.*, J. Alloys & Comp. **688**, 978-986 (2016).

[3] P. Čermák, *et al.*, in preparation.

[3] F. Ye, R. S. Fishman, J. A. Fernandez-Baca, *et al.*, PRB **83**, 140401(R) (2011).

[4] Y. Xiao, C. M. N. Kumar, S. Nandi, *et al.*, PRB **93**, 214428 (2016).